

A New Ultra High Strength Stainless Steel Strengthened by Various Coexisting Nanoprecipitates

W. Xu^{a,b,*}, P.E. J. Rivera-Díaz-del-Castillo^{b,#}, W. Yan^c, K. Yang^c, D. San Martín^d, L.A.I.
Kestens^e, S. van der Zwaag^b

^a *Materials Innovation Institute M2i, Kluyverweg 1, 2629 HS, Delft, The Netherlands,*

^b *Novel Aerospace Materials (NovAM) Group, Faculty of Aerospace Engineering, Delft
University of Technology, Kluyverweg 1, 2629 HS, Delft, the Netherlands,*

^c *Institute of Metal Research, Chinese Academy of Sciences, 72 Wenhua Road,
Shenyang, 110016, China,*

^d *Materialia Group, Department of Physical Metallurgy, Centro Nacional de
Investigaciones Metalúrgicas (CENIM-CSIC), Av. Gregorio del Amo 8, 28040 Madrid,
Spain, E-mail: dsm@cenim.csic.es*

^e *Department of Materials Science and Engineering, Ghent University, Technologiepark
903, 9052 Gent, Belgium.*

*# The author is now at Department of Materials Science and Metallurgy, University of
Cambridge, Pembroke Street, CB2 3QZ, Cambridge, United Kingdom.*

Keyword: maraging steels, stainless steels, thermodynamics, precipitation, alloy design.

Abstract

A general computational alloy design approach based on thermodynamic and physical metallurgical principles, and coupled with a genetic optimization scheme, is presented.

The model is applied to develop a new ultra high strength maraging stainless steel. The

alloy composition and heat treatment parameters are integrally optimised so as to achieve microstructures of fully lath martensite matrix strengthened by multiple desirable precipitates of MC carbides, Cu particles and Ni₃Ti intermetallics. The combined mechanical properties, corrosion resistance and identification of actual strengthening precipitates in the experimental steel grade produced on the basis of the model predictions provide a strong justification of the alloy design approach.

Introduction

Steels combining properties of ultra high strength (UHS), good ductility and corrosion resistance are of great importance in automotive, aerospace, nuclear, gear, bearing and other industries. They are the future key materials for lightweight engineering design strategies and corresponding CO₂ savings [1]. Various alloying elements such as C, Cr, Ni, Al, Ti, Mo, V, Mn, Nb, Co, Cu, W, Si, B and N, are combined in such alloy systems so as to obtain desirable microstructures and properties.

In UHS maraging steels, precipitate species may potentially cause the desired strengthening effect depending on the nature of precipitates and the distribution of their population in terms of size, density and spatial distribution. Obtaining the most desirable combination strongly depends on the precipitation thermokinetics and can be tailored through alloy composition and heat treatment. Out of the list of potential precipitates, MC carbide is a very effective strengthening precipitate which is usually composed by Ti, V and/or Nb and is stable and expected even in low C grades. They basically show two types of size distribution [2, 3]: (i) coarse (1-10 μm) and ineffective primary particles formed during solidification and (ii) fine (5-500 nm) and strength raising secondary precipitates. Under some conditions, a fraction of the primary MC

carbides can be dissolved during the austenitisation/solution heat treatment, and reprecipitate as fine secondary precipitates during the aging treatment or when these materials are subjected to high-temperature applications. The significant strengthening effect of MC carbides and effects of alloying elements have been reported for various steel grades [4-6]. On the other side, steel grades based on intermetallic precipitates, only contain a small amount of C in order to avoid the formation of carbides or carbonitrides but nevertheless reach a high strength level. Stiller *et al.* [7-9] studied the precipitation sequence in Nanoflex 1RK91[®]. The investigations showed a high density of Ni₃(Ti,Al) precipitates responsible for the significant strengthening effect when aged at 748 K. He *et al.* [10, 11] investigated precipitation behaviour in 19Ni-4Mo-2Ti maraging steel and found that, for the optimal ageing temperature of 753 K, moderately sized Ni₃Ti precipitates distribute uniformly in the martensite matrix, leading to an optimal combination of strength and fracture toughness. Moreover, the microstructure development in commercial PH15-5 stainless steel after different heat treatments has been studied by Habibi-Bajguirani *et al.* [12, 13]. Two stages of hardening have been identified which are associated to the formation of Cu clusters aged at 723 K and another spherical shaped Cu particle at higher ageing temperature 823-873 K. Isheim *et al.* [14] also reported a high number density (10^{24} m^{-3}) of Cu rich precipitates after aging at 763 K for 100 minutes in a metastable martensitic matrix leading to near-peak hardness. The study of precipitation sequence in Nanoflex 1RK91 [8, 9] also suggested that, on aging at 748 K, Cu is the only element which precipitates only after a few minutes. The fine Cu particles act as nuclei for Ni₃ (Ti,Al) precipitates during further ageing. Hättestrand *et al.* [15] also reported the co-existence of Cu and Ni₃Ti precipitate in alloy C455: at the early ageing stage, small densely distributed spherical precipitates rich in Cu, Ti and Ni were observed, after one hour the precipitates grew to rod sharp

and separation of Ni/Ti and Cu rich precipitates was observed and eventually Ni₃Ti are found to start coarsening after 2 hours.

UHS stainless steels strengthened by multiple precipitates combining MC carbides, Cu particles and intermetallics are very attractive in order to achieve mechanical and corrosion properties beyond the current high level. However, the composition and ageing treatment conditions for fostering the precipitation of each species are very different and the competitions/conflicts have to be compromised so as to design the alloy utilizing multiple precipitates. The classical experimental trial and error approach or statistics based artificial neural networks is no longer sufficient and a model more rooted in physical metallurgy is required. Recently, a theory guided computational alloy design model has been presented by Xu *et al.* [16-19] in which alloy composition and corresponding heat treatment parameters for UHS stainless steels are optimized integrally so as to achieve desirable microstructures within a genetic optimization framework. The model was applied to design exercises of UHS stainless steels utilising either MC carbide, Cu clusters and/or Ni₃Ti/NiAl precipitates. In the present work, the model is applied to design an alloy possessing multiple strengthening precipitates of MC carbide, Cu particles and Ni₃Ti intermetallics. The characterizations of the prototype alloy including mechanical properties, corrosion resistance and identifications of precipitates provide experimental justification for the alloy design approach.

Model description

The combination of ultra high strength and good toughness can be realised via uniformly dispersed fine precipitates in a lath martensite matrix. This microstructure is obtained via a two step heat treatment: solution treatment to achieve a homogenous and

fully austenitic state followed by quench to room temperature so as to generate the martensitic matrix microstructure, and further ageing at a modest temperature to allow precipitation of desirable species in this finely grained matrix structure. A schematic diagram of the heat treatment scheme is shown in Figure 1.

The solution treatment is aimed to dissolve precipitates/inclusions formed preceding the austenitisation treatment and obtain a homogeneous austenitic matrix. Depend on the alloy composition, various phases can be presented in the as cast condition, e.g. various carbides and δ -ferrite. The presences of those phases are normally deleterious to the mechanical properties and therefore it is desirable to start from a pure austenitic matrix and to obtain a fully martensitic structure upon quenching. The fully martensitic matrix can be further strengthened by ageing treatment, which promotes the formation of desirable precipitates, e.g. MC carbide, Cu clusters and Ni₃Ti intermetallics, with a desired dispersion of a dense network of nanosized particles. Moreover, a good corrosion resistance can be achieved by ensuring a sufficient Cr concentration in the matrix upon the completion of precipitation. Furthermore, while fostering the formation of desirable microstructures in the ageing treatment, the formation of phases limiting strength or toughness (e.g. M₂₃C₆, M₆C and M₇C₃, cementite, μ and χ phases) should be prevented.

In order to achieve the designed microstructures as described above, a computational alloy design model coupled with genetic algorithm has been developed and published elsewhere [16-19]. The alloy composition, as well as the austenitisation and the ageing temperature, are optimized to achieve the maximum precipitation strengthening contribution while fulfilling all go/nogo criteria along the entire heat treatment.

Following the algorithm shown in Figure 1, each candidate solution is evaluated step by step and each go/nogo criterion need to be fulfilled subsequently so as to proceed further assessments: 1) the key factor of martensitic transformation, the martensite start (Ms) temperature, is estimated using the model by Ishida [20] and enforced as a go/nogo criterion of ①Ms temperature being above 473 K. 2) The thermodynamic calculation is performed at the austenitisation temperature T_{Aus} . Two go/nogo criteria are imposed subsequently as ②equilibrium austenite volume fraction larger than 99% and ③the maximum level of primary carbides limited to 0.5 % in volume. 3) Thermodynamic equilibrium is calculated at the ageing temperature, T_{Age} , and two go/nogo criteria are enforced: ④the maximum allowed volume fraction for all unavoided undesirable phases together was arbitrarily set at 1% and ⑤a minimum of 12 wt% Cr in the matrix upon completion of the precipitation reactions is required so as to form the Cr-rich corrosion resistant film. 4) For candidate solution which fulfils all go/nogo criteria ①-⑤, the precipitation strengthening contribution of desired species is calculated as $\sigma_p \propto f_v^{1/2} r^{-1/2}$ [17], where f_v is the equilibrium volume fraction of the precipitate at the aging temperature T_{Age} and r is the critical precipitate nuclei size, which is inversely proportional to the thermodynamic driving force for the precipitation. The evaluation of single candidate solution as described above is embedded in a genetic optimization scheme in order to find the combined optimal alloy composition and heat treatment temperatures in an effective manner.

Application of the model

In order to incorporate complex interactions escaping intuitive analyses, steel compositions containing up to 13 alloying elements were considered: C, Cr, Ni, Ti, Mo, Al, Cu, Co, Nb, N, V, Mn and Si. The concentration of all alloying elements were

allowed to vary except for Mn (set at 0.5 wt%) and N (set at 0.01 wt%), as recommended to facilitate alloy production at the industrial scale. The candidate solution is represented in the genetic model as a chromosome which concatenates 11 variable concentrations together with the austenitisation and ageing temperatures (i.e. 13 genes), allowing for the simultaneous optimization of alloy composition, austenitisation and the ageing temperatures. Thermodynamic calculations were performed by ThermoCalc coupled with TCFE6 database and a tailored database for Ni/Ti-based precipitates. The concentrations and temperatures were varied within ranges based on financial and technological constraints (Table 1). Each component was allowed to take 32 potential concentrations by equally dividing its compositional range. The ageing temperature and austenitisation temperature were allowed to vary within the range of 693-848 K and 1223-1533 K with intervals of 5 and 10 K, respectively.

The model was applied to design UHS stainless steel alloys strengthened by MC carbide precipitate and the optimal composition with corresponding temperatures is shown in Table 1. The resulting alloy is hereon termed alloy CAR. It is very important to mention that, although the alloy is designed to maximize the precipitation strengthening contribution of MC carbides, the thermodynamic calculation on the optimal composition also predicts important amounts of other precipitates, e.g. Cu clusters and Ni₃Ti intermetallics. The molar percentages of MC, Cu and Ni₃Ti at the ageing temperature of 738 K are 0.93, 0.60 and 1.71, respectively. Considering comparable amounts of the three kinds of strengthening precipitates, the alloy CAR is therefore referred to here as a multiple precipitates strengthened maraging steel. It should also be noted that, the model also allows for designing steels strengthened by various precipitate species present at once, i.e. by maximizing the overall precipitate

strengthening contribution of supplied by different species. However, owing to the fact that the strengthening contribution is scaled with the precipitate nature (precipitate/matrix interfacial energy and young's modulus etc.), the strengthening contribution of the different precipitates cannot be arithmetically added, so it becomes difficult to quantify and compare their absolute strengthening contributions, and justify the best configuration for the different species.

Experimental procedures

The alloys were prepared in a vacuum induction melting furnace as ingots of approximately 25 kg. The ingots were vacuum melted, using high purity ingredients to achieve the best cleanliness. Phosphorus, Sulphur, Arsenic, Boron and Tin were controlled to the lowest possible levels. The melting temperature was kept relatively low at about 1773 K and the chamber was flushed with Argon. The ingots were ground to smoothen their surface, soaked at 1473 K for 2 hours and subsequently forged into a slab at a finishing temperature above 1173 K. The slabs were reheated to 1473 K for 2 hours, and subsequently hot rolled into plates of 15 mm thickness by 6 consecutive passes in the temperature range of 1323-1073 K, followed by air cooling. The chemical analysis of the experimental alloy is given in Table 1.

The as hot rolled material was subjected to various solution treatment conditions within the temperature range of 1373-1473 K and subsequently quenched to room temperature so as to achieve lath martensite matrix before ageing. The ageing treatments were conducted at 723, 773 and 823 K from 6 minutes up to one day, in a salt bath with neutral salt and followed by natural cooling. The tensile specimens were prepared along the longitudinal direction following ASTM standards. The tensile tests were performed

at room temperature at a strain rate of 10^{-3} /s. The Vickers hardness was measured with a load of 1 kg.

The microstructures were investigated by optical microscopy, scanning electron microscopy (SEM), transmission electron microscopy (TEM) in combination with energy dispersive spectroscopy (EDS). X-ray Diffraction (XRD) was also applied to identify phases. Optical microscopy and SEM were carried out on specimens etched with Villela's reagent. The TEM investigation was carried out with a Jeol JEM-2200 FS microscope operating at 200 kV. The TEM thin foils were firstly mechanically polished to approximately 50 μm in thickness. Electro-polishing was performed with a solution of 10% perchloric acid + 90% methanol maintained at 233 K and 12 V.

Electrochemical measurements of open circuit potential (OCP) and potentiodynamic polarisation (PP) were performed in order to characterise the corrosion resistance of alloy CAR. Corrosion resistance investigations were also performed on commercial reference alloys: standard stainless steels 304 and 316, non-stainless UHS 300M and Aermet 100 steels, and maraging stainless steel 1RK91. OCP and PP measurements were conducted in a 3.5% NaCl solution (pH 6, open to air) using a platinum counter electrode and a saturated calomel or Ag/AgCl/Cl⁻ (saturated KCl) reference electrode. After stabilisation of the OCP in the solution for 24 hours, the polarisation curves were obtained by scanning the potential from -0.5 V versus OCP to +1.0 V versus OCP.

Results

Microstructures

The microstructures on the cross-section perpendicular to the rolling direction were characterised after various solution treatment conditions. Typical optical micrographs after solution treatment at 1373 K for 15 minutes and 1423 K for 60 minutes are shown in Figures 2(a) and (b), respectively. The micrographs display homogeneous microstructures and indicate that prior austenite grains grow significantly with increasing solution treatment temperature and longer time, but invariably transform to lath martensite upon oil quench. In Figure 2(a), a significant amount of precipitates can be observed while after solution treatment at higher temperature and longer time. Figure 2(b) shows that the number of precipitates is significantly reduced. However, some particles still remain. An X-ray diffractogram of Figure 2(b) is shown in Figure 2(c) which reveals a martensitic matrix without detectable precipitates.

The solution treatment condition combining of a temperature of 1423 K and a time of 15 minutes was chosen for further ageing treatment. Considering the designed optimal ageing temperature of 738 K and optimal ageing temperature range of 753-798 K on existing counterparts, alloy CAR was subjected to ageing treatment at 723, 773 and 823 K, respectively, and times ranging from 6 minutes up to 1 day at each temperature. Figure 3(a) shows an optical micrograph after ageing at 723 K for 15 minutes. Apart from the primary precipitates located at the prior austenite grain boundaries (indicated by arrows), a few new small precipitates can be identified within martensite laths. With the progress of precipitation, the specimen after ageing at 773 K for 2 hours (Figure 3(b)) displays a much denser distribution of precipitates, along with a bigger size of a few hundred nanometres. After a prolonged ageing treatment at 823 K for 24 hours, the optical micrograph in Figure 3(c) still reveals a dense precipitate network and no

prominent coarsening was observed. Further investigation is required to identify the nature of the precipitates.

Mechanical properties

Figure 4(a-b) shows respectively the variation of strength and total elongation at fracture as a function of aging time at different temperatures for alloy CAR. The strength of the solution treated specimens is about 1 GPa, which is in agreement with the XRD in Figure 2(c) indicating a martensitic matrix. A good ductility of 14.7 % is observed in the as solution treated condition. During the ageing treatment, it displays very slight increase at the ageing time of 6 minutes, indicating slow precipitation strengthening kinetics, and the strength increases and ductility decreases with increase of the ageing temperature. With respect to ageing time, the strength increases but ductility decreases gradually at a temperature of 723 K resulting in an optimum strength of 1.6 GPa at 24 hours within the ageing times considered. At an ageing temperature of 773 K, the optimal time is one hour and prolonged ageing leads to a slight decrease in strength and an increase in elongation. The strengthening effect for an ageing temperature of 823 K seems to be less effective and reaches a maximum at 15 minutes resulting in a UTS of 1.27 GPa in combination with 16 % elongation. The hardness evolution with ageing treatment as shown in Figure 4(c) does not display consistency with the strength results: hardness increases monotonically with ageing time at 723 and 823 K, while the hardness reaches optimum after 1 hour at 773 K. The highest hardness is observed after ageing at 823 K for 24 hours in which the hardness is above 500 Hv. In terms of both strength and hardness, a slow strengthening kinetics was observed and significant strengthening effects can be achieved at longer ageing times.

Corrosion resistance

General corrosion potential - current density profiles obtained from potentiodynamic polarisation curves are presented in Figure 5. The pitting potential and current density are also indicated for stainless grades. The comparison of corrosion potential and current density shows that alloy 300M and Aement100 have very negative potential and high current because of their non-stainless nature. Alloy CAR clearly displays better general and pitting corrosion resistance to that of the existing reference steels such as alloy nanoflex 1RK91 and standard stainless steels 304 and 316. Moreover, for both general corrosion and pitting corrosion, the potentials become more negative and corrosion currents increase with longer ageing time which indicates an easier and faster corrosion kinetics. The decrease of corrosion resistance along with ageing time is a logical result of the precipitation and solute depletion of the matrix.

Discussion

Thermodynamic predictions

Thermodynamic equilibrium calculations were performed with both the design and actual alloy composition of alloy CAR, at various austenitisation and aging temperatures. The results are shown in Table 2. ThermoCalc calculations show that alloy CAR of its designed composition will yield 0.5 % of primary carbide at the designed austenitisation temperature of 1533 K which amount is exactly at the upper limit of the design criterion. However, the C concentration of the experimental alloy is higher than the designed value, which will promote higher fractions of primary carbide at the designed temperature of 1533 K (0.75 %) and at the actual solutionizing temperature of 1423 K (0.87 %). Nevertheless, apart from notable changes of primary carbide fractions (Table 1), there are no other undesirable phases (e.g. δ -ferrite) are

predicted. With respect to the ageing treatment, the amount of MC carbides is almost identical, regardless of the changes in composition and ageing temperatures. The effects of composition and temperature are more prominent regarding Ni₃Ti precipitation. The actual alloy displays a slightly smaller amount of Ni₃Ti in comparison to that predicted for the ideal composition at the designed ageing temperature of 738 K. The molar percentage decreases with the increase in ageing temperature and at 873K, no Ni₃Ti precipitates are predicted. The precipitation of Cu particles also displays similar but weaker temperature dependence. Concerning undesirable phases at the ageing condition, a small amount of austenite (0.84 %) is predicted at 738 K for the ideal composition while the actual composition should lead to 2.39 % which is beyond the controlled level. The amount of austenite increases with higher ageing temperatures and becomes significant at a temperature above 873 K. This suggests that reverted austenite may form which significantly influences the properties. Furthermore, it is important to note that the difference of primary carbide fraction and carbide fraction at the ageing stage, which is the amount of carbide precipitates forming during ageing, decreases significantly comparing ideal alloy (0.93-0.50) with actual alloy (0.96-0.75/0.87) which implies a smaller strengthening contribution from carbides in the experimental alloy.

Identification of precipitates

In order to identify precipitate characteristics of the prototype alloy, a prolonged ageing condition of 24 hours at a modest temperature of 773 K was selected to determine the nature of precipitates employing TEM microscopy in combination with EDS analysis. As shown earlier in Figure 3 (a-c), in addition to a few primary carbides distributed along prior austenite grain boundaries, a fresh distribution of spheroidal intragranular precipitates with an average size of 100-300 nanometres in diameter can be observed

after ageing treatment. An SEM-EDS analysis across such small precipitates was performed and the results shown in Figure 6 suggest that the precipitates are TiNbC carbides. This is in very good agreement with thermodynamic predictions and the design strategy of utilising TiNbC carbides as one of strengthening precipitates, although they are of a bigger size than desirable because the ageing condition investigated is sufficient for significant growth or coarsening to take place. The precipitation strengthening contribution of carbides will be more prominent if they are at a smaller size.

Finely dispersed species apart from TiNbC precipitates were also found in alloy CAR and an STEM image is shown in Figure 7(a). This phase forms a very dense network of nanoprecipitates lower than 10 nm which are homogeneously distributed in the lath martensite matrix. The high resolution TEM image shown in Figure 7(b) clearly reveals the spheroidal morphology of such ultra fine precipitates. EDS investigations were performed along the horizontal lines crossing the ultra fine precipitates in Figures 8 and 9. The corresponding concentration profiles of Ni, Ti and Cu are plotted below the STEM images. The EDS results in Figure 8 show that precipitates are mainly composed of Ni and Ti, and possibly display some segregation of Cu. The concentration profiles together with the predictions in Table 2 suggest that the precipitates are Ni₃Ti intermetallics. Moreover, the Ni₃Ti precipitates were found to be very resistant to coarsening since their sizes remained below 10 nm after ageing at 773 K for 24 hours and therefore can provide significant contribution to strength. The coarsening resistant feature of Ni₃Ti precipitates is consistent with experimental observations by Raabe [1, 21] and He [10, 11]. In addition to Ni₃Ti precipitates, the STEM-EDS results in Figure 9 show a precipitate which is mainly composed by Cu. The presence of Cu particle is

also predicted in Table 2 and its herring morphology of twinned fringes is very similar to that reported by Habibi-Bajguirani in PH15-5 maraging steels [12, 13]. Furthermore, it is very interesting to highlight that experimental observations in maraging steel 1RK91 showed Cu particles to be the first to form after only a few minutes at 748 K. They can act as potential nuclei and encourage the precipitation of Ni₃Ti intermetallics [7, 8]. Figure 8 displays some Cu concentration fluctuations but does not suggest clear Cu enrichment in the Ni₃Ti precipitate. The correlation of Ni₃Ti and Cu precipitates in alloy CAR needs further detailed investigations.

Alloys strengthened by multiple precipitates

The trial alloy CAR successfully achieves the design goal of a lath martensite strengthened by multiple desirable precipitates of MC carbides, Cu particles and Ni₃Ti intermetallics. The thermodynamic analysis can be applied to explore the temperature dependence of desirable precipitates, and hence provides a very effective route for optimizing the ageing treatment condition. The different precipitation kinetic features, i.e. temperature dependence, nucleation/growth/coarsening velocity, will further allow for ageing treatment optimization by tailoring the precipitate configuration: the alloy can be subjected to multiple steps of ageing treatment so as to promote, at each temperature, a specific species of desirable precipitates, without destroying desirable precipitates formed in the previous step or jeopardizing precipitation in the following ageing steps. Moreover, the integrated model with the capability of simultaneous design of alloy composition as well as heat treatment parameters, will further allow the alloy composition to be designed in such way that multiple precipitates can be formed subsequently at their specific corresponding ageing temperature, and hence further optimise mechanical properties.

Conclusions

The paper presents a general theory-guided computation alloy design methodology and characterizations of the designed prototype alloy. The composition and heat treatment parameters were designed by integrally applying the genetic design approach, so as to achieve microstructures of a fully martensitic matrix strengthened by multiple desirable precipitates of MC carbides, Cu particle and Ni₃Ti intermetallics.

The characterization of prototype alloy CAR showed that, after the austenitisation treatment and quench, the alloy CAR possesses a nearly full martensitic matrix, with a small amount of primary carbide. Moreover, after ageing treatment at 773 K for 24 hours, prototype alloy CAR displays complex precipitation characteristics: homogeneously distributed TiNbC carbides at size of 100-300 nm, very finely dispersed spheroid Ni₃Ti around 10 nm and some Cu particle less than 10 nm with twinned structure, which are precisely identical to the designed species and hence provides a solid proof for the computational alloy design approach presented.

Alloy CAR displays very strong precipitation strengthening capability with relatively slow precipitation kinetics and achieves an attractive combination of 1.6 GPa UTS with elongation of 9 % after ageing at 773 K for 24 hours. Moreover, both the general and pitting corrosion resistance of the prototype alloy CAR are superior to those of the existing commercial counterparts.

Acknowledgement

This research was carried out under the project number MC5.04192 in the framework of the Research Program of the Materials innovation institute M2i (www.m2i.nl), the formerly Netherlands Institute for Metals Research. The authors are grateful to Dr. V. Bliznuk (Ghent University, Belgium) for the support on TEM investigation and Dr. S.J. Garcia Espallargas (TUDelft, the Netherlands) for assistance in the corrosion potential measurement. Furthermore, we acknowledge the professional advice from Dr. P. Morris (Corus U.K.) in selecting the compositional ranges and in the interpretation of experiments.

Reference

- [1] Raabe D, Ponge D, Dmitrieva O, Sander B. *Scripta Materialia* 2009;60:1141.
- [2] Leitnaker JM, Bentley J. *Metall Trans A* 1977;8 A:1605.
- [3] Padilha AF, Schanz G, Anderko K. *Journal of Nuclear Materials* 1982;105:77.
- [4] Klueh RL, Hashimoto N, Maziasz PJ. *Scripta Materialia* 2005;53:275.
- [5] Gavriljuk VG, Berns H. *Materials Science Forum* 1999;318:71.
- [6] Miyata K, Omura T, Kushida T, Komizo Y. *Metallurgical and Materials Transactions A: Physical Metallurgy and Materials Science* 2003;34 A:1565.
- [7] Stiller K, Danoix F, Hättestrand M. *Materials Science and Engineering A* 1998;250:22.
- [8] Stiller K, Hättestrand M, Danoix F. *Acta Materialia* 1998;46:6063.
- [9] Stiller K, Hättestrand M, Danoix F. *Acta Materialia* 1998;46:6063.
- [10] He Y, Yang K, Sha W. *Metallurgical and Materials Transactions A: Physical Metallurgy and Materials Science* 2005;36:2273.
- [11] He Y, Yang K, Sha W, Cleland DJ. *Metallurgical and Materials Transactions A: Physical Metallurgy and Materials Science* 2004;35 A:2747.

- [12] Habibi-Bajguirani HR, Jenkins ML. *Philosophical Magazine Letters* 1996;73:155.
- [13] Habibi Bajguirani HR. *Materials Science and Engineering A* 2002;338:142.
- [14] Isheim D, Gagliano MS, Fine ME, Seidman DN. *Acta Materialia* 2006;54:841.
- [15] Hättestrand M, Nilsson JO, Stiller K, Liu P, Andersson M. *Acta Materialia* 2004;52:1023.
- [16] Xu W, Rivera-Díaz-del-Castillo PEJ, van der Zwaag S. *Computational Materials Science*. 2008;44 678.
- [17] Xu W, Rivera-Díaz-del-Castillo PEJ, van der Zwaag S. *Philosophical Magazine*. 2008;88:1825.
- [18] Xu W, Rivera-Díaz-del-Castillo PEJ, van der Zwaag S. *Computational Materials Science*. 2009;45:467.
- [19] Xu W, Rivera-Díaz-del-Castillo PEJ, van der Zwaag S. *Philosophical Magazine*. 2009;89:1647.
- [20] Ishida K. *Journal of Alloys and Compounds* 1995;220:126.
- [21] Raabe D, Ponge D, Dmitrieva O, Sander B. *Advanced Engineering Materials* 2009;11:547.

Table 1 Concentration ranges, designed and actual alloy compositions, predicted

Ms temperature and deigned heat treatment temperatures of alloy CAR.

Concentrations are in weight percent and temperatures are in K.

	C	Cr	Ni	Ti	Mo	Al	Cu	Co
Min	0.01	12.00	1.00	0.01	0.50	0.01	0.50	0.01
Max	0.30	20.00	15.00	2.00	10.00	2.00	2.00	2.00
Design	0.075	12.00	4.16	0.46	0.50	0.01	2.00	2.00
Actual	0.089	11.98	4.14	0.53	0.51	0.03	2.22	2.09
	Nb	N	V	Mn	Si	Fe	T _{Age}	T _{Aus}
Min	0.01	0.01	0.01	0.50	0.30	Bal.	693	1223
Max	1.00	0.01	1.00	0.50	1.00	Bal.	848	1533
Design	0.11	0.01	0.01	0.50	0.55	Bal.	738	1533
Actual	0.11	-	0.005	0.61	0.57	Bal.		

Table 2 Phase equilibrium fractions calculated by ThermoCalc on actual and designed compositions at various solution and ageing temperatures. The amounts of phases are in

molar percent.

	Comp.	T _{Aus}	Aus	MC	Ni ₃ Ti	Cu
Solution treatment	Design	1533	99.50	0.50	-	-
	Actual	1533	99.25	0.75	-	-
		1423	99.13	0.87	-	-
Ageing treatment	Design	738	0.84	0.93	0.60	1.71
	Actual	673	2.13	0.95	0.70	1.95
		738	2.39	0.96	0.36	1.94
		773	3.02	0.96	0.21	1.91
		873	12.15	0.97	0	1.74
		973	77.63	0.97	0	1.01

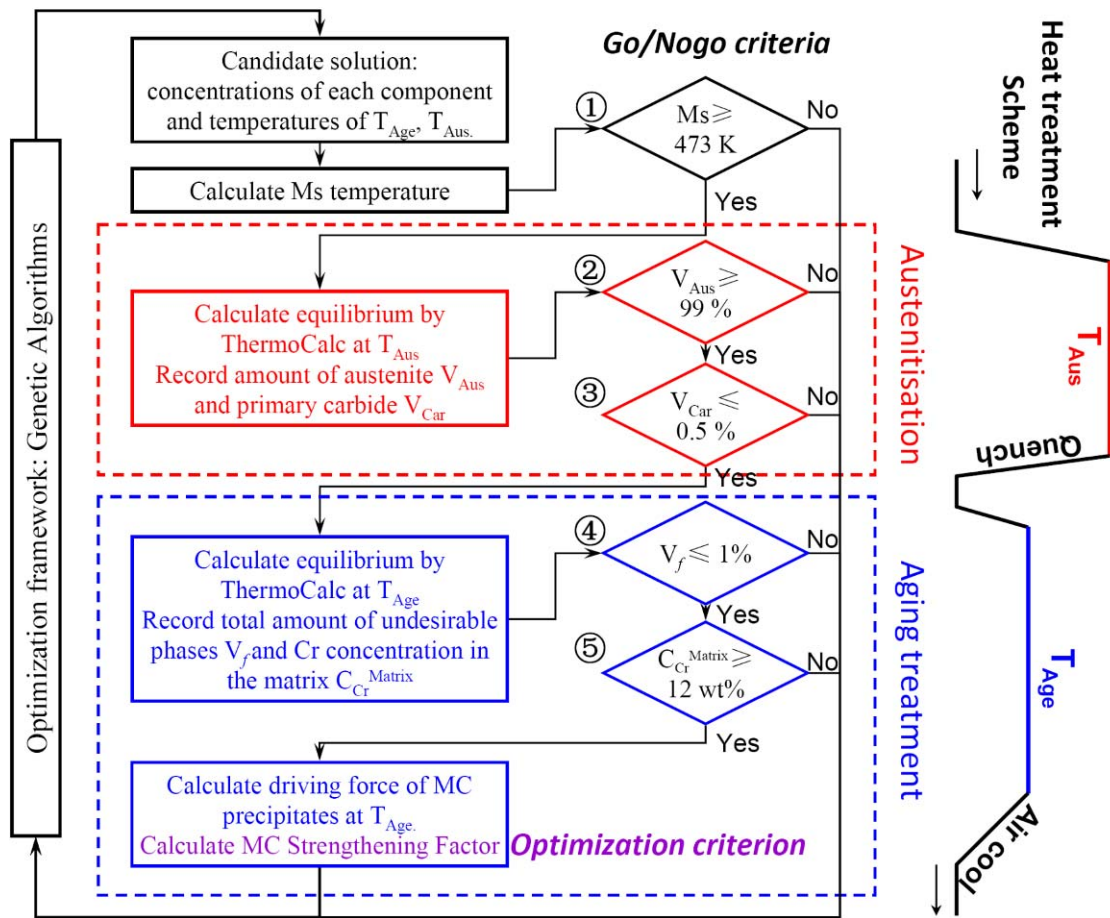


Figure 1 Schematic diagram of the heat treatment scheme and algorithm of the thermodynamic calculation and criteria evaluation.

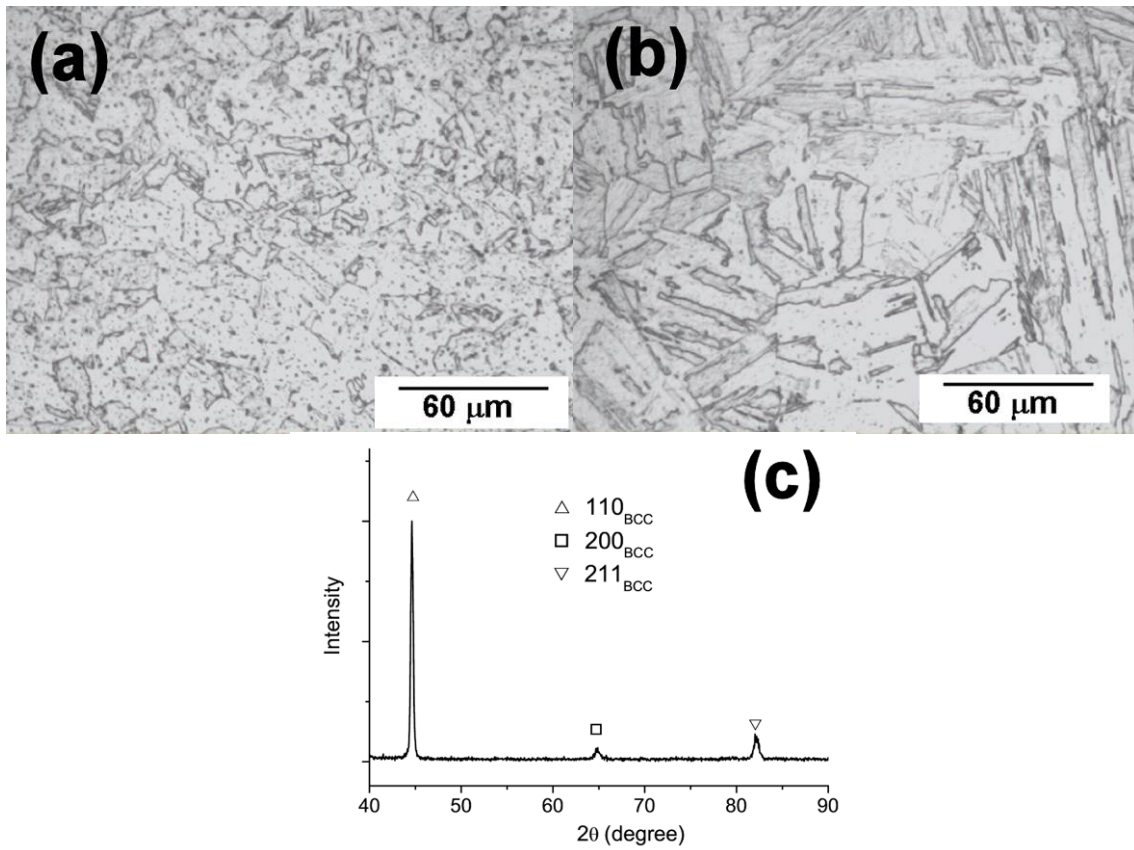


Figure 2 Optical micrographs on the cross section perpendicular to rolling direction of alloy CAR after solution treatment at 1373 K for 15 minutes (a) and at 1423 K for 60 minutes (b), followed by oil quench. (c) XRD diffractogram after solution treatment of (b).

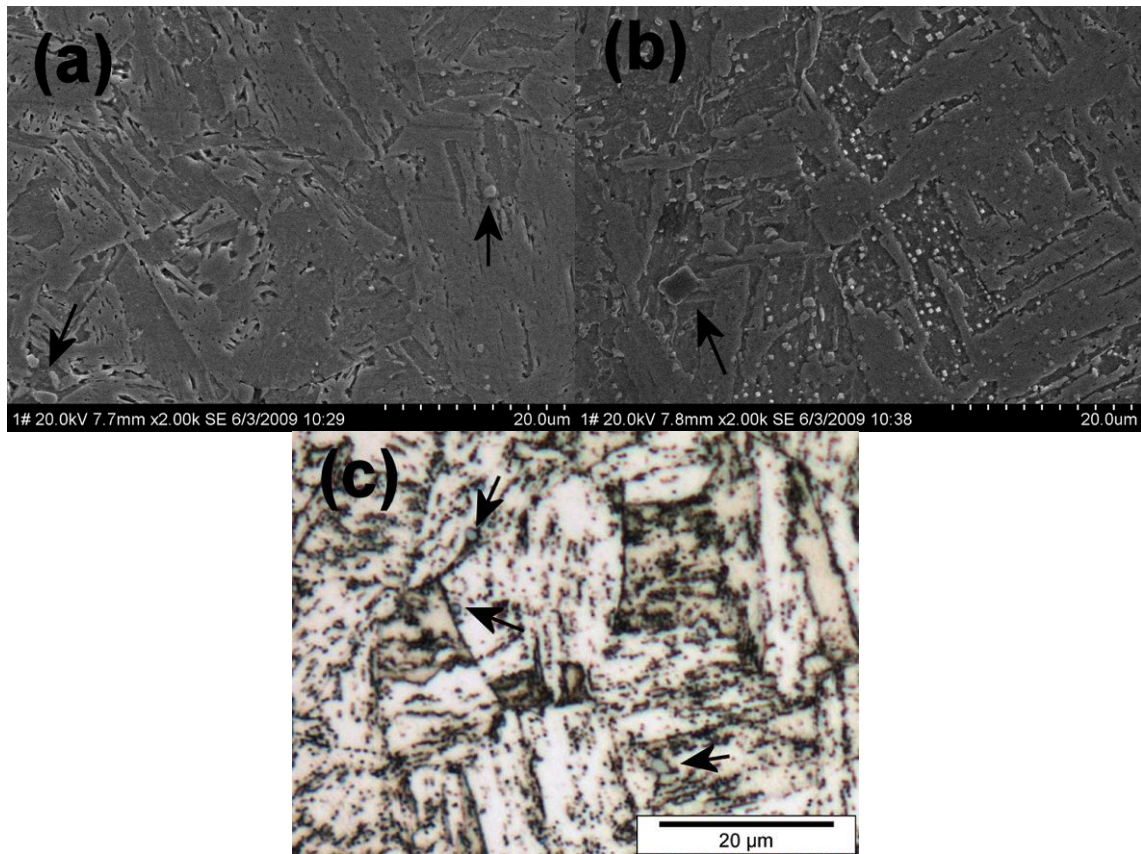


Figure 3 SEM and optical micrographs on the cross section perpendicular to rolling direction of alloy CAR after ageing treatment at (a) 723 K for 15 minutes, (b) 773 K for 2 hours and (c) 823 K for 24 hours.

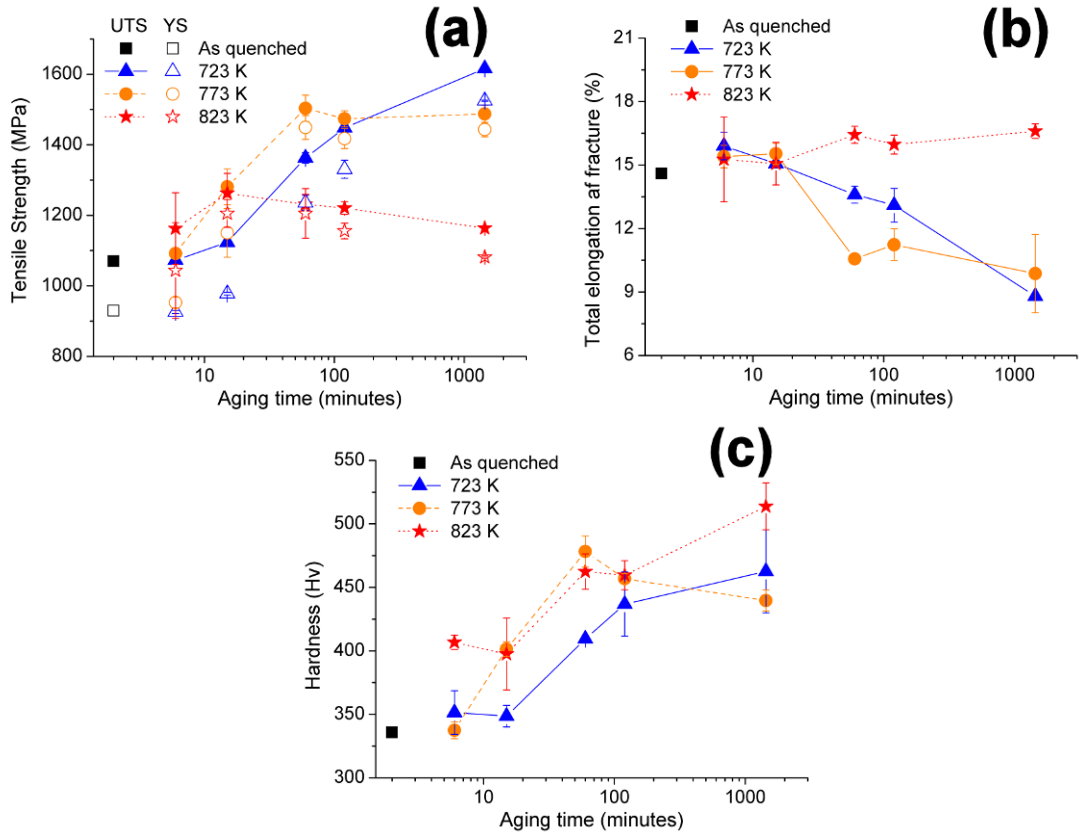


Figure 4 Variations of tensile strength (a), total elongation at fracture (b) and hardness (c) of alloy CAR with ageing time at aging temperatures of 723, 773 and 823 K, respectively.

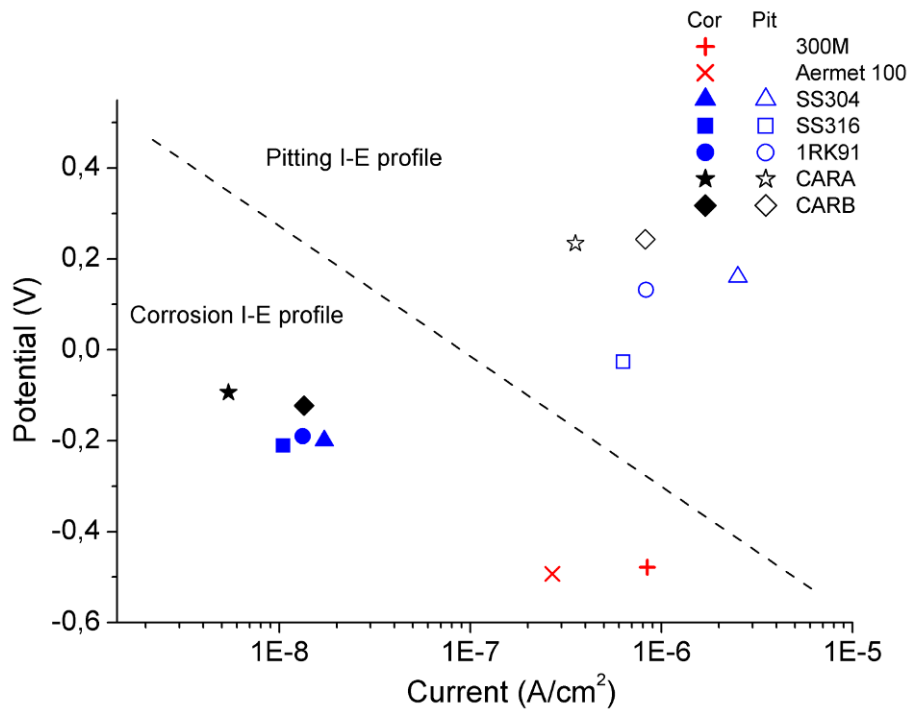


Figure 5 General corrosion potential-current density profiles and pitting corrosion potential - current density profiles of various alloys. For alloy CAR, the corrosion tests were performed after ageing at 773 K for 6 minutes (CARA) and 24 hours (CARB).

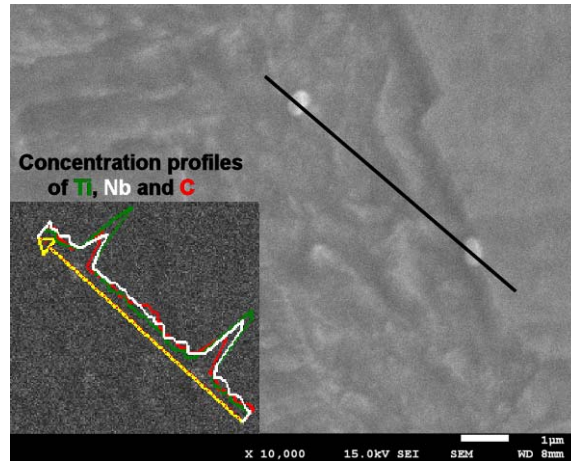


Figure 6 SEM micrographs of precipitates in alloy CAR after ageing at 773 K for 24 hours, with EDS results of concentration profiles of Ni, Ti, and C, measured on the line as indicated.

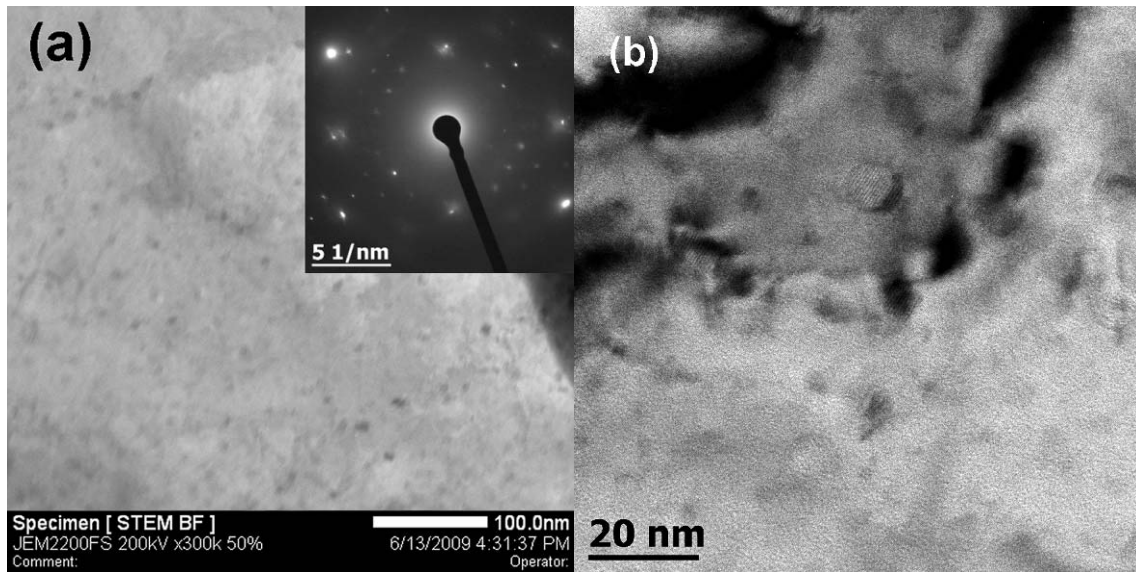


Figure 7 Micrographs of precipitates in alloy CAR after ageing at 773 K for 24 hours. (a) STEM image with diffraction pattern and (b) HRTEM image.

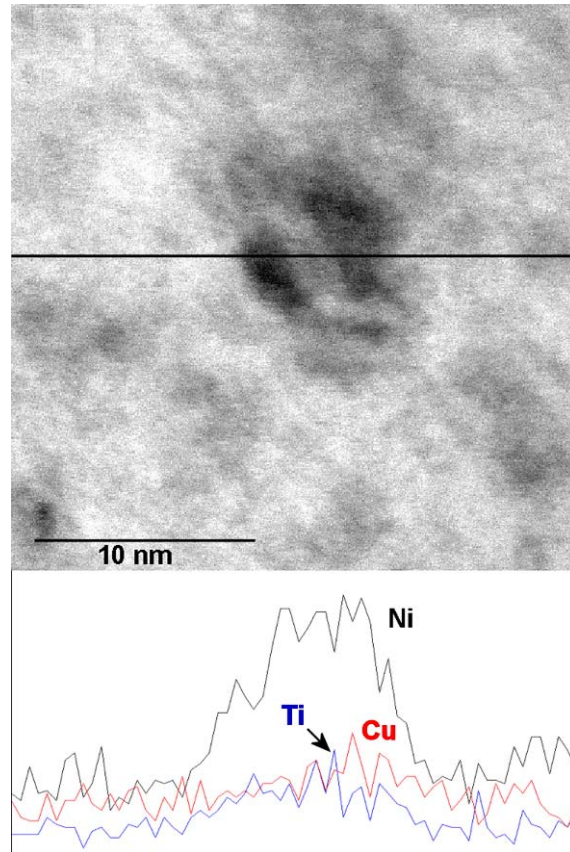


Figure 8 STEM micrograph of precipitates in alloy CAR after ageing at 773 K for 24 hours with EDS results of concentration profiles of Ni, Ti, and Cu, measured on the horizontal line as indicated.

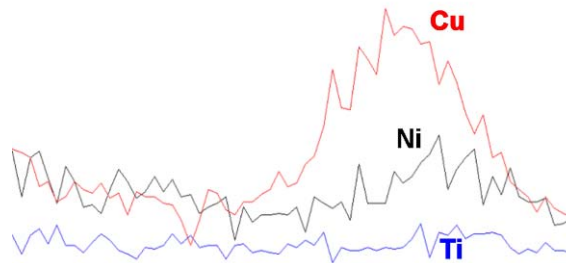
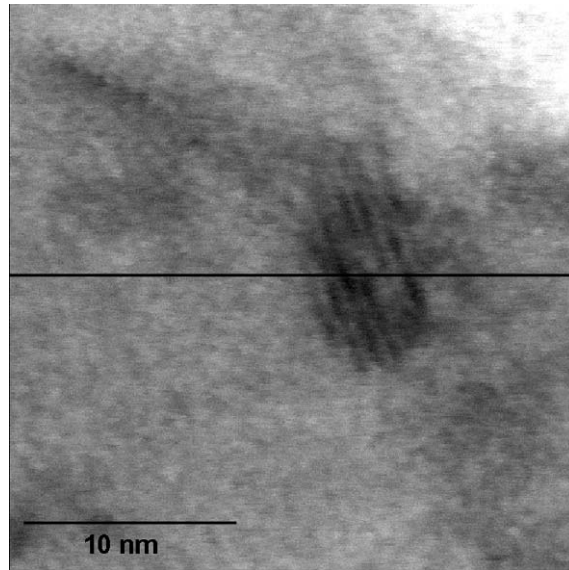


Figure 9 STEM micrograph of precipitates in alloy CAR after ageing at 773 K for 24 hours with EDS results of concentration profiles of Ni, Ti, and Cu, measured on the horizontal line as indicated.